ACS NANO

www.acsnano.org

ARTICLE

# All-in-One Nanowire Assay System for Capture and Analysis of Extracellular Vesicles from an *ex Vivo* Brain Tumor Model

Kunanon Chattrairat,* Takao Yasui,* Shunsuke Suzuki, Atsushi Natsume, Kazuki Nagashima, Mikiko Iida, Min Zhang, Taisuke Shimada, Akira Kato, Kosuke Aoki, Fumiharu Ohka, Shintaro Yamazaki, Takeshi Yanagida, and Yoshinobu Baba*

Cite This: *ACS Nano* 2023, 17, 2235−2244

Read Online

ACCESS | Metrics & More | Article Recommendations | Supporting Information

**ABSTRACT:** **Extracellular vesicles (EVs) have promising potential as biomarkers for early cancer diagnosis. The EVs have been widely studied as biological cargo containing essential biological information not only from inside vesicles such as nucleic acids and proteins but also from outside vesicles such as membrane proteins and glycolipids. Although various methods have been developed to isolate EVs with high yields such as captures based on density, size, and immunoaffinity, different measurement systems are needed to analyze EVs after isolation, and a platform that enables all-in-one analysis of EVs from capture to detection in multiple samples is desired. Since a nanowire-based approach has shown an effective capability for capturing EVs *via* surface charge interaction compared to other conventional methods, here, we upgraded the conventional well plate assay to an all-in-one nanowire-integrated well plate assay system (*i.e.*, a nanowire assay system) that enables charge-based EV capture and EV analysis of membrane proteins. We applied the nanowire assay system to analyze EVs from brain tumor organoids in which tumor environments, including vascular formations, were reconstructed, and we found that the membrane protein expression ratio of CD31/CD63 was 1.42-fold higher in the tumor organoid-derived EVs with a *p*-value less than 0.05. Furthermore, this ratio for urine samples from glioblastoma patients was 2.25-fold higher than that from noncancer subjects with a *p*-value less than 0.05 as well. Our results demonstrated that the conventional well plate method integrated with the nanowire-based EV capture approach allows users not only to capture EVs effectively but also to analyze them in one assay system. We anticipate that the all-in-one nanowire assay system will be a powerful tool for elucidating EV-mediated tumor−microenvironment crosstalk.**

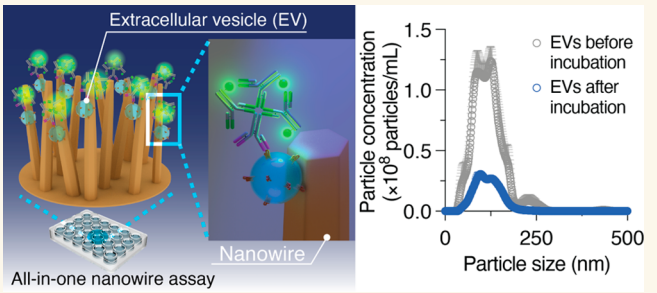


**KEYWORDS:** *extracellular vesicle, nanowire, brain tumor, organoid, membrane protein*

Extracellular vesicles (EVs; diameters of 30−2000 nm) are membrane vesicles containing nucleic acids, proteins, and bioactive lipids and provide intercellular communication and cellular function regulation.[1,2] Malignant cells, such as tumors, are known to have a higher amount of EV secretion with disease-related genetic and proteomic information than normal cells;[3−7] thus, EVs have been considered as a source of biomarkers for chronic diseases including some cancer types.[8−10] Some brain tumors are asymptomatic and are often already growing at the time of diagnosis; therefore, an ordinary diagnosis may delay detection and reduce survival rates.[11] Tumor cell-derived EVs have been reported to be a potential source of cancer biomarkers.[12−14] Thus, tumor organoid-derived EVs are expected to retain the biological information on the tumor as cultured in a three-dimensional (3D) cell culture, that is, an environment close to that of the tumor *in vivo*.[15] Hence, analysis of tumor organoid-derived EVs could lead to the discovery of brain tumor biomarkers. In this study, we conceived an idea to demonstrate the analysis of EVs derived from brain tumor organoids in the search for EV markers for brain tumors.

The first step in EV analysis is to capture EVs from biological samples.[16−18] Due to the biological, chemical, and

Received: August 26, 2022
Accepted: January 4, 2023
Published: January 19, 2023

Downloaded via UNIV OF TOKYO on April 15, 2023 at 01:33:18 (UTC).
See https://pubs.acs.org/sharingguidelines for options on how to legitimately share published articles.

© 2023 The Authors. Published by American Chemical Society

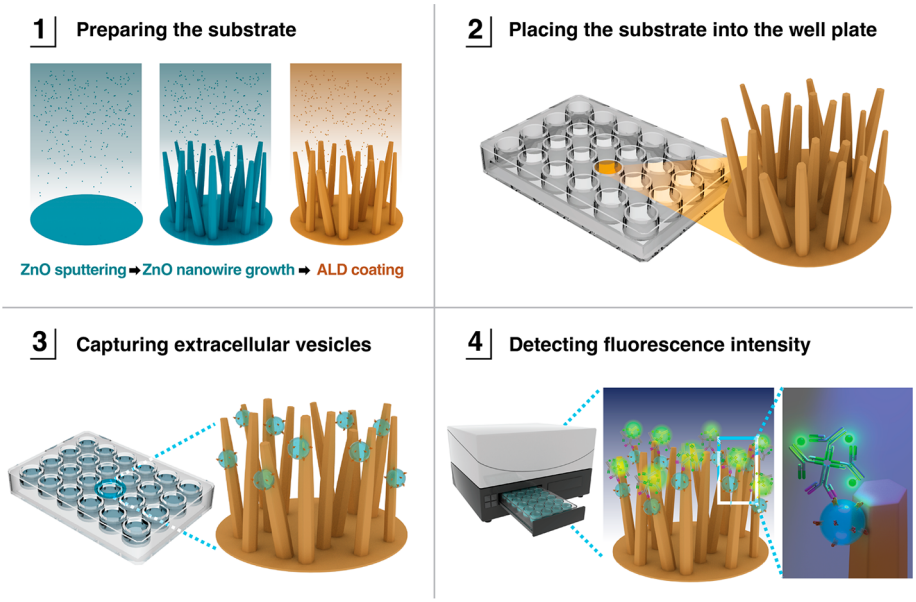


**Figure 1. Schematic images of EV capture and membrane protein measurement system. The ZnO nanowires were fabricated on a quartz substrate utilizing a sputtering method; then surface modification was carried out by coating them with a metal oxide by ALD. The substrate with growth nanowires was placed into each well of a well plate. Subsequently the EVs were captured based on surface charge. The EV membrane proteins were fluorescently detected, and biomarkers of brain tumors were searched for.**

physical properties of EVs, *e.g.*, their existence in a wide range of nanosize particles, at low concentrations and at high heterogeneities,[19−22] various capture methods for EVs from biological samples have been proposed. The conventional methodologies for EV capture are density-based capture using ultracentrifugation or differential centrifugation, immunoaffinity-based capture using specific membrane proteins, for example, CD9, CD63, and CD31, and size-based capture using size exclusion chromatography.[23,24] Additionally, alternative methodologies for EV capture are introduced, *e.g.*, microfluidic-based approaches by viscoelastic flow, filtration, aptamer-mediated sorting, and acoustic isolation and polymer precipitation.[25−28] Previously, we proposed a nanowire-based capture approach that could capture EVs in a charge-based manner from urine and the cell supernatant.[29−32]

The second step in EV analysis is to analyze specific EVs among the captured EVs.[33−35] Conventional EV capture platforms require measurement systems to obtain biological compositions that reflect body, cellular, and organ information. To obtain the specific biological EV information, membrane proteins on EVs are normally analyzed by immunoassay after solidification of the EVs,[36] by Western blotting after lysis treatment,[37] by a nanoplasmon-enhanced scattering assay,[38] and by mass spectrometry for peptide information.[39] The nanowire-based capture approach has the advantages of rapid and simple operation with high EV yield, the ability to discover massive numbers of microRNAs (miRNAs), and the ability to obtain the correlation between surface charge and membrane proteins.[29,30,32]

Here, we developed an all-in-one nanowire assay system suitable for both EV capture and analysis, instead of multiple conventional methods, to search for EV markers from a small amount of the cell supernatant of brain tumor organoids and urine samples. Previously, we demonstrated that the ZnO (bare) nanowire has an ability to capture EVs based on the surface charge, and we obtained a correlation between the surface charge and the expressed proteins on the EVs.[29] The results showed that a correlation existed between EV capture efficiency and charge surface of three types of nanowires (ZnO (bare), ZnO/$TiO_2$ (core/shell), and ZnO/$SiO_2$ (core/shell)), and the correlation illustrated that a stronger positively charged surface could provide higher EV capture efficiency than a weakly positively charged surface could. Thus, the ZnO (bare) nanowires, which are the strongest positively charged surface among the three types, showed the highest EV capture efficiency.[29] In this work, we used ZnO/$Al_2O_3$ (core/shell) nanowires, which provide a stronger positively charged surface than ZnO (bare) nanowires to capture EVs, and subsequently we detected EV membrane proteins. To efficiently implement EV capture and EV analysis of membrane proteins, we upgraded the conventional well plate assay to an all-in-one nanowire-integrated well plate assay system (*i.e.*, a nanowire assay system) suitable for both EV capture and membrane protein measurement (Figure 1). Finally, we applied the nanowire assay system to brain tumors to search for cancer-related biomarkers of EV membrane proteins from a small sample volume.

## RESULTS AND DISCUSSION

**The Nanowire Assay System for Capturing EVs Based on Surface Charge.** To integrate both capturing and analyzing of EVs in one assay system for an easy-to-use and powerful EV analysis methodology, we combined a conventional well plate assay and nanowire-based EV capture as the all-in-one nanowire assay system. Figure 1 shows schematic images of the EV capture and the EV membrane protein measurement system. We fabricated nanowire substrates by synthesizing ZnO nanowires on fused silica substrates utilizing the hydrothermal method. Furthermore, different metal oxides, $Al_2O_3$, $SiO_2$, and $TiO_2$, were deposited on the ZnO nanowires by atomic layer deposition (ALD) to obtain the core−shell structure, and then, the nanowire substrates were placed onto a 24-well plate. The EVs in phosphate-buffered saline (PBS) (Figures 2 and 3), cell- and organoid-derived EVs in culture


https://doi.org/10.1021/acsnano.2c08526
ACS Nano 2023, 17, 2235−2244

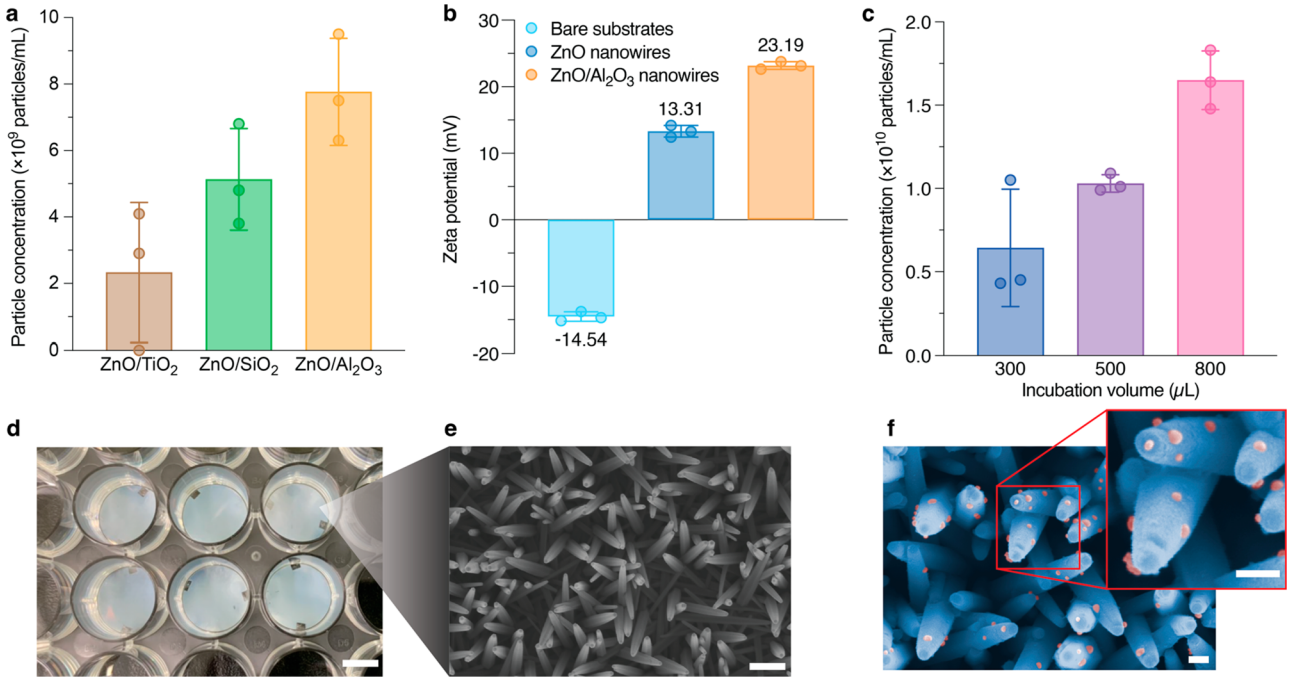


**Figure 2. Nanowire assay system capture of EVs. (a) EV capture concentration on different oxide nanowires with an initial concentration of $2.29 \times 10^{10}$ particles/mL, calculated by using $C_0 - C$, where $C_0$ is the initial concentration of EVs and $C$ is the uncaptured concentration of EVs. Error bars show the SD for an individual experiment ($N = 3$). (b) Zeta potential of bare substrates, ZnO (bare) nanowires, and ZnO/$Al_2O_3$ (core/shell) nanowires. Error bars show the SD for an individual experiment ($N = 3$). (c) EV capture concentration with different incubation volumes. Error bars show the SD for an individual experiment ($N = 3$). (d) Photo showing the ZnO/$Al_2O_3$ (core/shell) nanowires on a quartz substrate in the 24-well plate; scale bar, 10 mm. (e) FESEM image of ZnO/$Al_2O_3$ (core/shell) nanowires; scale bar, 400 nm. (f) FESEM image of captured EVs (colored in pink) on ZnO/$Al_2O_3$ (core/shell) nanowires (colored in blue); scale bar, 200 nm. A zoom-in image is also shown for the red square area; scale bar, 200 nm.**

media (Figure 4), and EVs in urine (Figure 4) were incubated to capture EVs on the nanowires *via* charge-based capture. Finally, EV membrane protein profiling was carried out by utilizing antibody fluorescence detection, which is an easy to implement and rapid method.

For EV membrane protein profiling, here, core−shell structure nanowires were used to capture EVs based on surface charge. Scanning transmission electron microscopy (STEM) images and energy dispersive X-ray spectroscopy (EDS) elemental mappings (Figures S1 and S2) confirmed that the core−shell structure was obtained for the ZnO/$Al_2O_3$ nanowires. The capture concentration was calculated by using $C_0 - C$ where $C_0$ is the initial concentration of EVs, *i.e.*, the EV concentration before dropping EVs in PBS onto the nanowire well plate, and $C$ is the uncaptured concentration of EVs, i.e., the EV concentration after collecting EVs in PBS from the nanowire well plate. These ZnO/$Al_2O_3$ (core/shell) nanowires showed the highest capture concentration of EVs, $7.77 \times 10^9$ particles/mL (Figure 2a), whereas ZnO/$SiO_2$ (core/shell) nanowires and ZnO/$TiO_2$ (core/shell) nanowires captured EVs at concentrations of $5.13 \times 10^9$ and $3.50 \times 10^9$ particles/mL, respectively, which were 66% and 45% of the EVs captured by the ZnO/$Al_2O_3$ (core/shell) nanowires. Previously we demonstrated that the ZnO (bare) nanowires could capture EVs with the highest capture efficiency *via* charge-based interaction compared to ZnO/$SiO_2$ and Zn/$TiO_2$ (core/shell) nanowires, which had a negatively charged surface, and that the charge surface potential of the nanowire also affected the EV capture efficiency.[29] In this work, the ZnO/$Al_2O_3$ (core/shell) nanowires had the strongest positively charged surface, and this charged surface affected the charge-based capture (Figure 2b), which led to the higher EV capture concentration of ZnO/$Al_2O_3$ (core/shell) nanowires among core−shell structure nanowires (Figure 2a). Although the EV capture concentration was decreased with a decrease of sample volume, the EV capture concentration was as high as $6.40 \times 10^9$ particles/mL at 300 $\mu$L (Figure 2c), which is enough for further EV membrane protein analysis.

To evaluate the EV capture concentration in the nanowire assay system, the nanowire surface area and number of nanowires were calculated. ZnO/$Al_2O_3$ (core/shell) nanowires were fabricated on a quartz substrate and placed into a 24-well plate (Figure 2d; surface area of 1.86 $cm^2$). Analysis of field emission scanning electron microscopy (FESEM) images showed that the nanowires had an average diameter of 111 nm ($N = 100$), average height of 1.81 $\mu$m ($N = 100$), and average density of 25 nanowires/$\mu m^2$ ($N = 20$ images) (Figure 2e). The number of nanowires could be estimated as $4.66 \times 10^9$ nanowires in the fabricated area, and it resulted in around a 16-fold larger surface area compared to the bare substrate. The large number of nanowires in the present nanowire assay system was enough to capture and immobilize EVs on nanowires by charge-based interaction in biological samples, as generally, EV concentrations are $10^9$−$10^{10}$ particles/mL.[20,40,41] Thus, due to the 300 $\mu$L required volume for our nanowire assay system, the number of EVs in the well plate assay were approximately $3.0 \times 10^8$ to $3.0 \times 10^9$, and we concluded that the number and surface area of the nanowires in the well plate assay system were enough to capture EVs from biological samples. Furthermore, we demonstrated that the EVs were captured on ZnO/$Al_2O_3$ (core/shell) nanowires on the basis of the FESEM image results (Figure 2f).



https://doi.org/10.1021/acsnano.2c08526
ACS Nano 2023, 17, 2235−2244

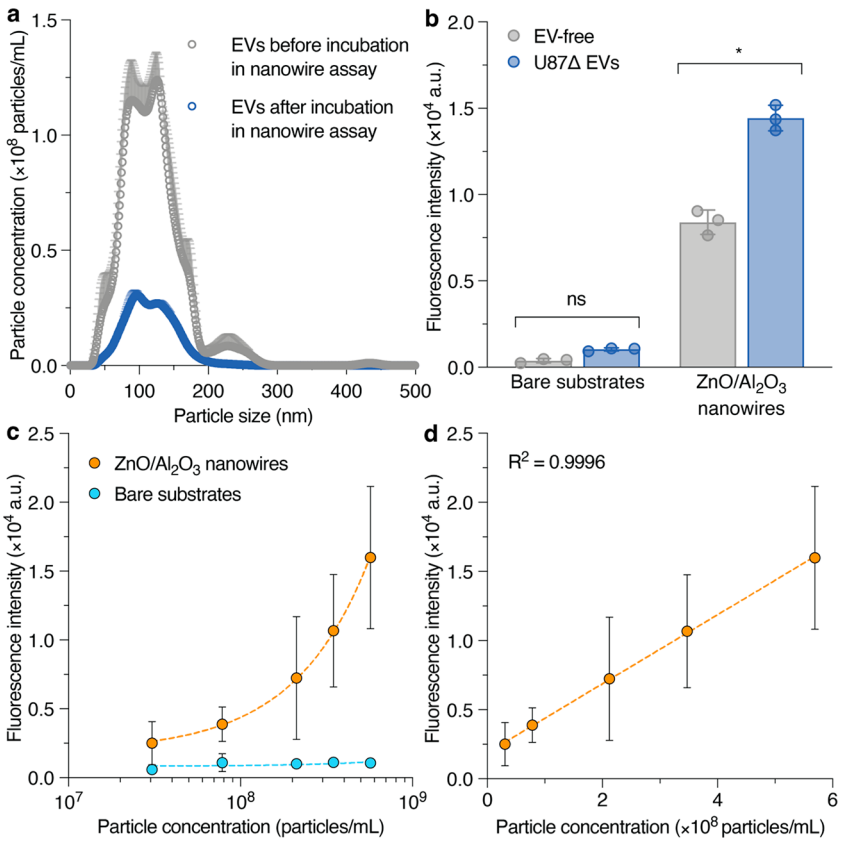


**Figure 3. CD63 profiling from captured cell-derived EVs in PBS prepared by ultracentrifugation in the nanowire assay system. (a) Size distribution of EVs in PBS before and after incubation in the nanowire assay system. Error bars show the SD for an individual experiment ($N$ = 3). (b) Fluorescence intensity of CD63 profiling of EV-free PBS and U87Δ EVs in PBS using a bare quartz substrate and ZnO/$Al_2O_3$ (core/shell) nanowires. Error bars show the SD for an individual experiment ($N$ = 3), and the $p$-value was calculated by an unpaired Mann−Whitney test (*, $p$ < 0.05; ns, not significant). (c) EV concentration versus CD63 fluorescence intensity using a bare quartz substrate and ZnO/$Al_2O_3$ (core/shell) nanowires. The dashed lines show the linear regression (orange, ZnO/$Al_2O_3$ (core/shell) nanowires; blue, bare quartz substrate). (d) The calibration curve of EV concentration versus CD63 fluorescence intensity using ZnO/$Al_2O_3$ (core/shell) nanowires with $R^2$ = 0.9996. In (c) and (d), error bars show the SD for an individual experiment ($N$ = 3).**

**Captured EV Membrane Protein Profiling in Nanowire-Based Assay System for Cells, Organoids, and Urine Samples.** For EV analysis with the nanowire assay system, the cell- and organoid-derived EVs were captured, and membrane protein profiling was performed with CD63 fluorescent-labeled antibody. To obtain higher sensitivity of the membrane protein fluorescence detection,[42] both primary antibodies and secondary fluorescent-labeled antibodies were used (Figure S3) rather than just primary fluorescent-labeled antibodies, and the results indicated there was a significant increase of fluorescence intensity (Figure S4). We targeted the CD63 membrane protein as the marker for EVs for the following reasons: high enrichment of CD63 has been observed in small extracellular vesicles and was shown to be instrumental in formation of small intraluminal vesicles,[43,44] and a correlation has been reported between CD63 fluorescence intensity and EV concentration in the case of EV capture by nanowires.[29] When the fluorescence intensity of the CD63 membrane protein was compared between the bare substrate and ZnO/$Al_2O_3$ (core/shell) nanowires, ZnO/$Al_2O_3$ (core/shell) nanowires provided higher fluorescence intensity, and 1.7-fold higher fluorescence intensity was obtained compared to the EV-free PBS due to the high EV capture concentration with the charge-based interaction (Figures 3a and 3b).[29−31] Moreover, our nanowire assay system was verified with various combinations of presence and absence of ZnO/$Al_2O_3$ (core/shell) nanowires, EVs, and antibodies (Figure S5), and the results showed that the nanowire assay system could capture EVs *via* measurement of CD63 with high fluorescence intensity.

Furthermore, a relationship between the EV concentration ranging from 3.06 × $10^7$ to 5.69 × $10^8$ particles/mL and fluorescence intensities was considered, and a marked correlation was observed between the concentration of captured EVs and their fluorescence intensity (Figure 3c). In addition, the calibration curve of the captured EV concentration versus fluorescence intensity with our nanowire assay system was plotted, and the linear regression with $R^2$ = 0.9996 was obtained (Figure 3d). Next, the limit of detection (LOD) of 1.25 × $10^7$ particles/mL was achieved based on the 3$\sigma$ method. Considering the reported EV capture and analysis methods, we concluded that the nanowire assay system in this study has the advantages of simultaneous EV capture and detection in the same plate, no need for an antibody as the capture probe, and a sufficient LOD for further tumor diagnosis and prognosis (Table 1). Although some of the reported EV capture methods have lower LODs, the nanowire assay system is advantageous with respect to being a simple method and a no immunoaffinity-capture required method. Previous research studies reported the capture of the EVs *via*


https://doi.org/10.1021/acsnano.2c08526
ACS Nano 2023, 17, 2235−2244

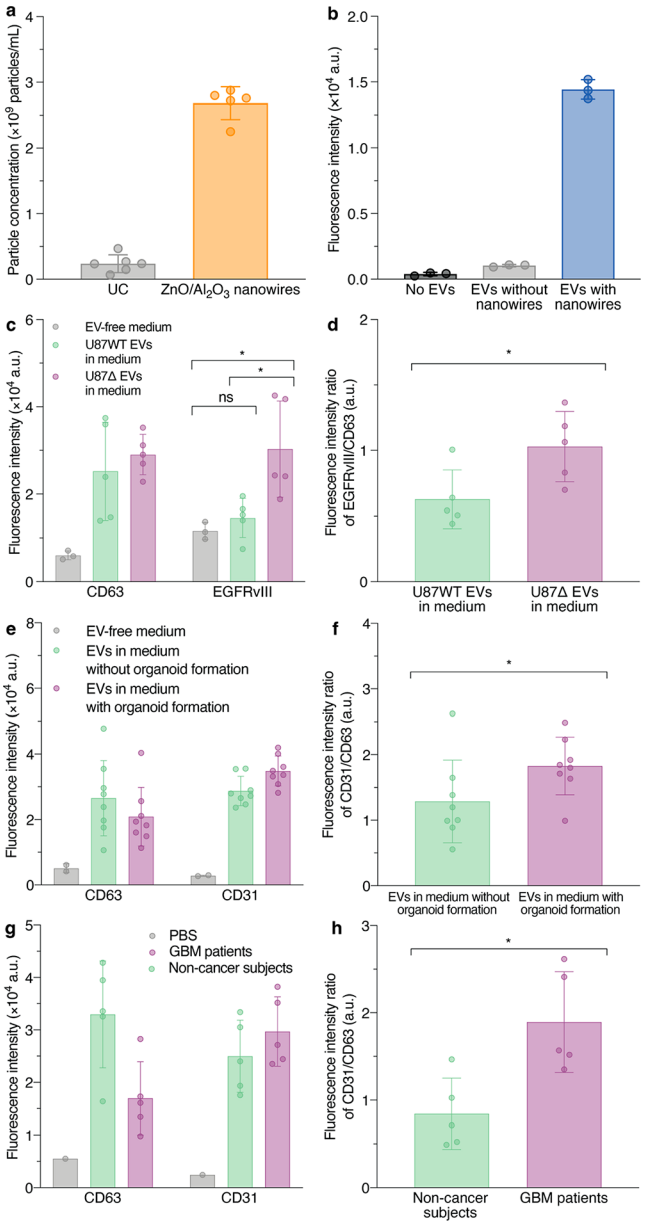


**Figure 4. Membrane protein profiling of EVs for cell, organoid, and urine samples. (a) Particle concentration captured from 300 $\mu$L of medium: comparison between the ultracentrifugation (UC) method and $ZnO/Al_2O_3$ (core/shell) nanowires. Error bars show the SD for an individual experiment ($N \geq 5$). (b) CD63 fluorescence measurement for PBS on a 24-well plate (no EVs), EVs in PBS prepared by ultracentrifugation on a 24-well plate without nanowires (EVs without nanowires), and EVs in cell culture medium on a 24-well plate with nanowires (EVs with nanowires). Error bars show the SD for an individual experiment ($N = 3$). (c) Fluorescence intensity obtained using the nanowire assay system for CD63 and EGFRvIII membrane protein profiling of EV-free medium and U87WT EVs and U87Δ EVs in medium. (d) Fluorescence intensity ratio of EGFRvIII/CD63 of U87WT EVs and U87Δ EVs in medium. (e) Fluorescence intensity obtained using the nanowire assay system for CD63 and CD31 membrane protein profiling of EV-free medium and EVs in medium without and with organoid formation. (f) Fluorescence intensity ratio of CD31/CD63 of EVs in medium without and with organoid formation. (g) Fluorescence intensity obtained using the nanowire assay system for CD63 and CD31 membrane protein profiling of EVs in urine samples from glioblastoma (GBM) patients and noncancer subjects. (h) Fluorescence intensity ratio of CD31/CD63 of EVs in urine samples from glioblastoma (GBM) patients and noncancer subjects. (c–h) Error bars show SD for an individual experiment ($N \geq 5$); the $p$-value was calculated by an unpaired Mann–Whitney test (*, $p < 0.05$; ns, not significant).**

surface biomarkers such as CD9, CD63, CD81, *etc.*;[45−49] however, nonspecific capture could provide an opportunity to capture more information about EVs compared to partial capture by immunoaffinity.[50] Furthermore, since generally the EV concentrations are $10^9$ to $10^{10}$ particles/mL,[20,40,41] the nanowire assay system is expected to be able to detect EVs in biological fluids. And, the nanowire assay system uses the advantage of charge-based interaction for EV capture accompanied by the conventional well plate method, which leads to simple EV capture and detection in only one assay system. Therefore, the nanowire assay system is feasible for further practical applications in tumor diagnosis and prognosis.

We captured and analyzed not only cell-derived EVs but also brain tumor organoid-derived EVs and urine samples from glioblastoma patients and noncancer subjects. Before performing EV membrane protein analysis, we compared particle capture concentrations from 300 $\mu$L of medium between the ultracentrifugation method and our nanowire assay. The captured particle concentration of our nanowire assay ($2.68 \times 10^9$ particles/mL) was 17.8-fold higher than that of the ultracentrifugation method ($1.5 \times 10^8$ particles/mL) under the same conditions (Figure 4a). A similar reduction in size distribution was observed when EVs were captured from 300 $\mu$L of medium without ultracentrifugation, and this reduced distribution was comparable to the size distribution of EVs collected by ultracentrifugation (Figure S6). Furthermore, the fluorescence intensity of CD63 on our nanowire assay was significantly higher than that of CD63 fluorescence intensity when ultracentrifugally collected EVs were incubated in 24-well plates for 20 h (Figure 4b). These results clearly showed that our nanowire assay system can capture a large number of EVs from biological samples, and the captured EV sizes are comparable to the collected EV sizes by ultracentrifugation.

EGFRvIII has been widely used as a glioblastoma biomarker that is frequently observed in tumor progression; however, EGFRvIII is unstable and leads to varying expressions.[51,52] In a 2D cell culture, U87Δ, engineered glioblastoma cells, showed stable and high expression of EGFRvIII, whereas U87WT, wild-type glioblastoma cells, showed low expression of EGFRvIII comparable to an EV-free medium (Figure 4c).[53] Moreover, we analyzed the expression ratio of EGFRvIII/CD63, and the ratio showed a statistically significant difference of expression between U87WT and U87Δ; this demonstrated the unstable expression of EGFRvIII (Figure 4d). Considering the correlation of CD63 fluorescence intensity to EV concentration of EVs obtained from different cell lines[29] and the correlation of CD63 fluorescence intensity to EV concentration of EVs obtained from a single cell line (Figure 3d), it would be possible to express the EV concentration in terms of CD63 fluorescence intensity. Using the expression ratio in each sample, we could observe a change of membrane protein expression level.

To further understand brain tumor organoid-derived EVs, the brain tumor organoid formation was cultured by the 3D cell culture technique, which provided a pure tumor


https://doi.org/10.1021/acsnano.2c08526
ACS Nano 2023, 17, 2235−2244

Table 1. Comparison of EV Capture and Analysis Methods

| method | sample | capture approach | required instrument | LOD (particles/mL) | required volume (mL) | captured particle (particles) | ref |
|---|---|---|---|---|---|---|---|
| microchip | ultracentrifuged cell (MCF-7) medium | immunoaffinity | fluorescence microscope | $6.30 \times 10^{10}$ | 0.002 | $1.26 \times 10^{8}$ | 61 |
| dot blotting | spiking cancer-cell-derived EVs (OVCAR-3) in blood plasma | immunoaffinity | manual pin microarray spotter and fluorescence microscope | $3.10 \times 10^{5}$ | 0.006 | $1.86 \times 10^{3}$ | 62 |
| 3D nanopatterned EV-CLUE chip | ultracentrifuged-purified EVs (MDA-MB-231) | immunoaffinity | fluorescence microscope | $5 \times 10^{5}$ | 0.006 | $3 \times 10^{3}$ | 48 |
| immunization and membrane filters | ultracentrifuged cell (MCF-10A, MDA-MB-231, and SK-BR-3) medium and spiking EVs in EV-free serum | immunoaffinity and chemisorption | chemiluminescence substances and microplate reader | $1.00 \times 10^{4}$ | 0.1 | $8.27 \times 10^{1}$ | 63 |
| single particle interferometric reflectance imaging sensor | ultracentrifuged cell (HEK-293) medium and human cerebrospinal fluid | immunoaffinity | single particle interferometric reflectance imaging sensor | $3.94 \times 10^{9}$ | 0.02 | $7.88 \times 10^{7}$ | 64 |
| DNA-capped single-wall carbon nanotube aptasensor | ultracentrifuged cell (MCF-7) medium | immunofluorescence | UV−vis spectrophotometry | $5.20 \times 10^{5}$ | 87.2 | $4.53 \times 10^{7}$ | 65 |
| nanowire assay system | organoid medium and glioblastoma patient urine | charge-based interaction | well plate reader | $1.25 \times 10^{7}$ | 0.3 | $3.75 \times 10^{6}$ | this work |

composition for analysis (Figure S7). A 3D cell culture, less artificial than a 2D cell culture, has been demonstrated as able to mimic the cell microenvironment and obtain practical information about cell-to-cell interactions and metabolic profiling in research studies of stem cells and various types of diseases.[54−56] Several research studies have reported that the CD31 expression in vasculogenesis has a correlation with brain tumor grade and prognosis through epithelial to mesenchymal transitions (EMTs).[57−59] Although the fluorescence intensity of CD31 had high expression in the medium both with and without organoid formation (Figure 4e), the expression ratio of CD31/CD63 showed a significant *p*-value, and we could propose CD31 as a brain tumor biomarker (Figure 4f). Furthermore, urine samples from glioblastoma patients and noncancer subjects were analyzed by our nanowire assay system. The expression ratio of CD31/CD63 of EVs in urine samples showed a statistically significant difference between glioblastoma patients and noncancer subjects, which was the same trend as seen for brain tumor organoids (Figures 4g and 4h). Our results demonstrated that our nanowire assay system is a good candidate for effective capture and analysis of EV membrane proteins in future cancer diagnosis applications, and additionally, the results confirmed that CD31 has a good potential for use as a brain tumor biomarker.

## CONCLUSION

In summary, we demonstrated a nanowire EV capture integrated measurement system that has the ability to capture EVs *via* charge-based interaction and to achieve membrane protein profiling of EVs from biological samples. The positive charge of $ZnO/Al_2O_3$ (core/shell) nanowires plays an important role in EV capture and membrane protein profiling (CD63, EGFRvIII, and CD31). Our methodology provided an effective assay system for EV capture and membrane protein profiling with linear regression and had the LOD of $1.25 \times 10^7$ particles/mL. To improve the LOD, we hypothesized that longer nanowires and/or coating with a stronger positively charged surface could capture a greater number of EVs and provide lower LOD. Moreover, our nanowire assay system showed its potential to provide a feasible indicator of the EV membrane proteins for brain tumor organoids, although further experimental analysis is needed to confirm the biomarker. Since the present methodology allows users to capture EVs and profile EV membrane proteins in one assay system, our nanowire assay system offers an opportunity to develop a powerful tool for cancer diagnosis with high precision and accuracy.

## EXPERIMENTAL SECTION

**Ethics Approval and Consent to Participate.** The present study was approved by the institutional review board at Nagoya University Hospital (approval number: 2012-0067) and complied with all provisions of the World Medical Association Declaration of Helsinki. Tumor samples were collected intraoperatively upon receiving informed consent from the patients.

**Cell Culture and EV Purification.** U87 cell lines were cultured in Dulbecco's modified Eagle's medium (DMEM, Thermo Fisher Scientific Inc.) with 10% exosome-depleted fetal bovine serum (FBS, System Biosciences, LLC) containing 1% penicillin−streptomycin (PS, Thermo Fisher Scientific Inc.). Before collecting EVs from cells, the medium was changed to advanced DMEM (Thermo Fisher Scientific Inc.). In each passage, $3 \times 10^6$ cells were seeded into 15 mL of cell medium in a culturing flask and cultured in an incubator (Panasonic Corp.) at 37 °C and in a 5% $CO_2$ atmosphere. The cell


https://doi.org/10.1021/acsnano.2c08526
ACS Nano 2023, 17, 2235−2244

culture medium was collected and centrifuged (10 min, 4 °C, 300*g*), and the medium was collected again and further centrifuged (10 min, 4 °C, 2000*g*). Then, the medium was filtered through a 0.22 μm filter (Merck Millipore Ltd.). Next, the filtered medium was ultracentrifuged (80 min, 4 °C, 110000*g*). After discarding the supernatant, 6 mL of 0.22 μm filtered PBS (Thermo Fisher Scientific Inc.) was added to wash the collected EVs, followed by ultracentrifuging again (80 min, 4 °C, 110000*g*). After discarding the supernatant, 1 mL of 0.22 μm filtered PBS was added to collect the EVs, which were then stored at 4 °C. The EVs in PBS collected by ultracentrifugation were used to calculate EV capture concentration on different oxide nanowires, detect CD63 membrane protein, and obtain the calibration curve as a proof-of-concept (Figures 2 and 3), whereas EVs in medium were used for the comparison analysis between ultracentrifugation and nanowires and EV membrane protein profiling of brain tumor cells and brain tumor organoids (Figure 4). EVs in urine were also used for EV membrane protein profiling (Figure 4).

**Generation of Tumor Organoids.** Fresh surgically resected tissues were immediately minced into 1 $mm^3$ pieces and put into DMEM culture medium (Thermo Fisher Scientific Inc.) supplemented with 10% FBS (System Biosciences, LLC) and 1% PS (Thermo Fisher Scientific Inc.) or serum-free culture medium (neurobasal medium, N-2, B-27, PS (Thermo Fisher Scientific), recombinant human FGF protein (50 ng/mL), and recombinant human EGF protein (50 ng/mL; R&D Systems). To remove red blood cells and debris, the pieces were incubated in 5 mL of organoid culture medium, containing 15 μL of ACK lysing buffer (Thermo Fisher Scientific Inc.) and 5 μL of type IV collagenase (Thermo Fisher Scientific Inc.) at room temperature, and then mechanically dissociated by pipetting. Dissociated cells were resuspended in Matrigel basement membrane matrix (Corning Inc.), which was diluted with the same amount of culture medium. Then, 350 μL of the suspended Matrigel mixture was seeded in each well of a six-well plate, incubated for 30 min at 37 °C and 5% $CO_2$ atmosphere, and then overlaid with 2 mL of the organoid culture medium. The culture medium was refreshed every few days. The collected organoid medium was briefly centrifuged (10 min, 4 °C, 300*g*, and then 10 min, 4 °C, 3000*g*) to remove apoptotic bodies[60] and filtered using a 0.22 μm filter (Merck Millipore Ltd.) before incubating in the nanowire assay.

**EV Preparation for Urine Samples.** After urine samples were collected from glioblastoma patients and noncancer subjects, the urine samples were centrifuged (10 min, 4 °C, 300*g*, and then 10 min, 4 °C, 3000*g*) to remove apoptotic bodies,[60] and then they were filtered through a 0.22 μm filter (Merck Millipore Ltd.). Next, the filtered urine samples were incubated in the nanowire assay system according to the procedure (Figure S3).

**Nanowire Fabrication and Characterization.** We used a radio frequency sputterer (Sanyu Electron Co., Ltd.) to deposit a ZnO layer on quartz substrates (Crystal Base, Japan; 15.4 mm diameter, 0.13 mm thickness) before growing the ZnO nanowires. The ZnO nanowires were grown by the hydrothermal method at 95 °C for 3 h using 70 mL of growth solution containing 30 mM of both hexamethylenetetramine (HMTA) (Wako Pure Chemical Industries, Ltd.) and zinc nitrate hexahydrate ($Zn(NO_3)_2{\cdot}6H_2O$) (Thermo Fisher Scientific Inc.). Then, a layer of $Al_2O_3$, $TiO_2$, or $SiO_2$ was deposited on the as-grown ZnO nanowires by an ALD apparatus (Ultratech Inc.). This modified the ZnO nanowire surface to ZnO/$Al_2O_3$, ZnO/$TiO_2$, or ZnO/$SiO_2$ nanowires as the core−shell structure (Figure 1). The morphology and composition of ZnO (bare) and ZnO/$Al_2O_3$ (core/shell) nanowires were characterized by FESEM, STEM, and EDS (JEOL Ltd., Figures S1 and S2). For the cross-sectional SEM-EDS analysis, we utilized an accelerating voltage of 15 kV. For the single-nanowire STEM-EDS analysis, we used an accelerating voltage of 30 kV. The EDS mapping images were 512 × 384 pixels, and the delay time for each pixel was 0.1 ms. The images were integrated over 100 cycles. The peaks of Zn K$\alpha$ (8.630 keV), O K$\alpha$ (0.525 keV), and Al K$\alpha$ (1.487 keV) were chosen to construct the elemental mapping images. The zeta potential of the nanowires was measured by using a commercial apparatus (Otsuka Electronics Co., Ltd.).

**EV Capture and Membrane Protein Measurement on Nanowires.** We utilized the conventional well plate with nanowire substrates placed in the wells (Figure 1). EV concentrations were analyzed using a nanoparticle tracking analysis (NTA) instrument (Malvern Panalytical, Ltd.). Video data were collected five times for a 60 s time period each time. Camera level and detection threshold were set to 13 and 5, respectively. NanoSight NTA 3.2 software was used for data analysis. The capture concentration was calculated by using $C_0 - C$, where $C_0$ is the initial concentration of EVs, *i.e.*, the EV concentration before dropping EVs in PBS onto the nanowire well plate, and $C$ is the uncaptured concentration of EVs, *i.e.*, the EV concentration after collecting EVs in PBS from the nanowire well plate. The EVs captured on nanowires were coated with platinum film by using a plasma exposure system (Vacuum Device Inc.) to a thickness around 10 nm for imaging with an FESEM apparatus (Carl Zeiss AG). To profile the EV membrane proteins, 300 μL of medium containing EVs was added onto the nanowire substrate placed in each well, where incubation was carried out for 20 h at 37 °C, after which the solution was discarded (Figure S3). The same incubation time was used for the well plate experiment without nanowires. Next, 300 μL of blocking solution (KPL 10% BSA blocking solution, SeraCare) was added to a well followed by incubation for 1 h at 37 °C. After that, a washing step was performed three times with 150 μL of PBS. We used anti-human CD63 antibody (Cosmo Bio Co., Ltd.), anti-human EGFRvIII antibody (Biorbyt), or anti-human CD31 antibody (Abcam plc.) as the primary fluorescence antibody. Then, the secondary fluorescence antibody was used for anti-CD63, anti-EGFRvIII, and anti-CD31, respectively, as fluorescein isothiocyanate (FITC)-conjugated Affinipure goat anti-mouse antibody (Proteintech Group Inc.), FITC-conjugated goat anti-mouse IgG2a antibody, and Alexa Fluor 467-conjugated goat anti-rabbit IgG H&L (Abcam plc.). The fluorescence measurements were made using a commercial well plate reader (Tecan Trading AG). Then, for all fluorescence intensity measurements, the fluorescence measurement region of the well was divided into 12 sections, from which the same one region was used to detect the fluorescence intensity of all membrane proteins.

## ASSOCIATED CONTENT

### Supporting Information

The Supporting Information is available free of charge at https://pubs.acs.org/doi/10.1021/acsnano.2c08526.

(1) FESEM image, STEM image, and EDS elemental mappings of ZnO (bare) nanowires; (2) FESEM and STEM images and EDS elemental mappings of ZnO/$Al_2O_3$ (core/shell) nanowires; (3) schematic drawing of the experimental procedures; (4) fluorescence measurement of CD63 membrane protein profiling of EV-free and U87Δ EVs in medium with FITC-labeled secondary antibody; (5) CD63 fluorescence measurement for nanowire assay system verification; (6) size distribution of EVs; (7) photos of brain tumor organoid (PDF)

## AUTHOR INFORMATION

### Corresponding Authors

**Takao Yasui** − *Department of Biomolecular Engineering, Graduate School of Engineering, Nagoya University, Nagoya 464-8603, Japan; Japan Science and Technology Agency (JST), PRESTO, Kawaguchi, Saitama 332-0012, Japan; Institute of Nano-Life-Systems, Institutes of Innovation for Future Society, Nagoya University, Nagoya 464-8603, Japan;* orcid.org/0000-0003-0333-3559; Email: yasui@chembio.nagoya-u.ac.jp

**Kunanon Chattrairat** − *Department of Biomolecular Engineering, Graduate School of Engineering, Nagoya*

*University, Nagoya 464-8603, Japan;* orcid.org/0000-0001-7587-6777; Email: kunanon.chat@gmail.com

**Yoshinobu Baba** − *Department of Biomolecular Engineering, Graduate School of Engineering, Nagoya University, Nagoya 464-8603, Japan; Institute of Nano-Life-Systems, Institutes of Innovation for Future Society, Nagoya University, Nagoya 464-8603, Japan; Institute of Quantum Life Science, National Institutes for Quantum and Radiological Science and Technology, Inage-ku, Chiba 263-8555, Japan;* Email: babaymtt@chembio.nagoya-u.ac.jp

### Authors

**Shunsuke Suzuki** − *Department of Biomolecular Engineering, Graduate School of Engineering, Nagoya University, Nagoya 464-8603, Japan*

**Atsushi Natsume** − *Institute of Nano-Life-Systems, Institutes of Innovation for Future Society, Nagoya University, Nagoya 464-8603, Japan*

**Kazuki Nagashima** − *Japan Science and Technology Agency (JST), PRESTO, Kawaguchi, Saitama 332-0012, Japan; Department of Applied Chemistry, Graduate School of Engineering, The University of Tokyo, Bunkyo-ku, Tokyo 113-8656, Japan;* orcid.org/0000-0003-0180-816X

**Mikiko Iida** − *Department of Biomolecular Engineering, Graduate School of Engineering, Nagoya University, Nagoya 464-8603, Japan*

**Min Zhang** − *Department of Biomolecular Engineering, Graduate School of Engineering, Nagoya University, Nagoya 464-8603, Japan*

**Taisuke Shimada** − *Department of Biomolecular Engineering, Graduate School of Engineering, Nagoya University, Nagoya 464-8603, Japan*

**Akira Kato** − *Institute of Nano-Life-Systems, Institutes of Innovation for Future Society, Nagoya University, Nagoya 464-8603, Japan*

**Kosuke Aoki** − *Institute of Nano-Life-Systems, Institutes of Innovation for Future Society, Nagoya University, Nagoya 464-8603, Japan;* orcid.org/0000-0002-3274-5272

**Fumiharu Ohka** − *Department of Neurosurgery, School of Medicine, Nagoya University, Nagoya 466-8550, Japan*

**Shintaro Yamazaki** − *Department of Neurosurgery, School of Medicine, Nagoya University, Nagoya 466-8550, Japan*

**Takeshi Yanagida** − *Department of Applied Chemistry, Graduate School of Engineering, The University of Tokyo, Bunkyo-ku, Tokyo 113-8656, Japan*

Complete contact information is available at: https://pubs.acs.org/10.1021/acsnano.2c08526

### Author Contributions

K. Chattrairat contributed to formal analysis, investigation, visualization, writing the original draft, and writing review and editing. T. Yasui contributed to conceptualization, funding acquisition, methodology, project administration, supervision, and writing review and editing. S. Suzuki and M. Iida contributed to analysis, investigation, and methodology. A. Natsume contributed to analysis and materials. K. Nagashima contributed to analysis and investigation. Z. Min, T. Shimada, A. Kato, K. Aoki, F. Ohka, S. Yamazaki, and T. Yanagida all contributed to analysis. Y. Baba contributed to conceptualization, funding acquisition, project administration, and supervision.

### Notes

The authors declare no competing financial interest.

## ACKNOWLEDGMENTS

This research was supported by the Japan Science and Technology Agency (JST) PRESTO (JPMJPR19H9), JST SICORP (JPMJSC19E3), the New Energy and Industrial Technology Development Organization (NEDO) JPNP20004, the JSPS Grant-in-Aid for Scientific Research (S) 18H05243, the JSPS Grant-in-Aid for Scientific Research (B) 21H01960, the JSPS Grant-in-Aid for Exploratory Research 20K21124, the JSPS Grant-in-Aid for Transformative Research Area (A) 21H05778, the Medical Research and Development Program (AMED Grant Nos. JP21he2302007 and JP21zf0127004), and the Cooperative Research Program of the "Network Joint Research Center for Materials and Devices". We also thank Dr. H. Yukawa, Dr. D. Onoshima, and Dr. A. Arima for their valuable discussions.

## REFERENCES

(1) Xu, K.; Liu, Q.; Wu, K.; Liu, L.; Zhao, M.; Yang, H.; Wang, X.; Wang, W. Extracellular Vesicles As Potential Biomarkers and Therapeutic Approaches in Autoimmune Diseases. *J. Transl. Med.* **2020**, *18*, 432.

(2) Clayton, A.; Boilard, E.; Buzas, E. I.; Cheng, L.; Falcon-Perez, J. M.; Gardiner, C.; Gustafson, D.; Gualerzi, A.; Hendrix, A.; Hoffman, A.; Jones, J.; Lasser, C.; Lawson, C.; Lenassi, M.; Nazarenko, I.; O'Driscoll, L.; Pink, R.; Siljander, P. R.; Soekmadji, C.; Wauben, M.; et al. Considerations Towards a Roadmap for Collection, Handling and Storage of Blood Extracellular Vesicles. *J. Extracell. Vesicles* **2019**, *8*, 1647027.

(3) Rabinowits, G.; Gercel-Taylor, C.; Day, J. M.; Taylor, D. D.; Kloecker, G. H. Exosomal MicroRNA: a Diagnostic Marker for Lung Cancer. *Clin. Lung Cancer* **2009**, *10*, 42−46.

(4) Logozzi, M.; De Milito, A.; Lugini, L.; Borghi, M.; Calabro, L.; Spada, M.; Perdicchio, M.; Marino, M. L.; Federici, C.; Iessi, E.; Brambilla, D.; Venturi, G.; Lozupone, F.; Santinami, M.; Huber, V.; Maio, M.; Rivoltini, L.; Fais, S. High Levels of Exosomes Expressing CD63 and Caveolin-1 in Plasma of Melanoma Patients. *PLoS One* **2009**, *4*, No. e5219.

(5) O'Brien, K.; Rani, S.; Corcoran, C.; Wallace, R.; Hughes, L.; Friel, A. M.; McDonnell, S.; Crown, J.; Radomski, M. W.; O'Driscoll, L. Exosomes from Triple-Negative Breast Cancer Cells Can Transfer Phenotypic Traits Representing Their Cells of Origin to Secondary Cells. *Eur. J. Cancer* **2013**, *49*, 1845−1859.

(6) Melo, S. A.; Sugimoto, H.; O'Connell, J. T.; Kato, N.; Villanueva, A.; Vidal, A.; Qiu, L.; Vitkin, E.; Perelman, L. T.; Melo, C. A.; Lucci, A.; Ivan, C.; Calin, G. A.; Kalluri, R. Cancer Exosomes Perform Cell-Independent MicroRNA Biogenesis and Promote Tumorigenesis. *Cancer Cell* **2014**, *26*, 707−721.

(7) Willms, E.; Johansson, H. J.; Mager, I.; Lee, Y.; Blomberg, K. E.; Sadik, M.; Alaarg, A.; Smith, C. I.; Lehtio, J.; El Andaloussi, S.; Wood, M. J.; Vader, P. Cells Release Subpopulations of Exosomes with Distinct Molecular and Biological Properties. *Sci. Rep.* **2016**, *6*, 22519.

(8) Lane, R. E.; Korbie, D.; Hill, M. M.; Trau, M. Extracellular Vesicles As Circulating Cancer Biomarkers: Opportunities and Challenges. *Clin. Transl. Med.* **2018**, *7*, 14.

(9) Ramirez-Garrastacho, M.; Bajo-Santos, C.; Line, A.; Martens-Uzunova, E. S.; de la Fuente, J. M.; Moros, M.; Soekmadji, C.; Tasken, K. A.; Llorente, A. Extracellular Vesicles As a Source of Prostate Cancer Biomarkers in Liquid Biopsies: a Decade of Research. *Br. J. Cancer* **2022**, *126*, 331−350.

(10) Weng, J.; Xiang, X.; Ding, L.; Wong, A. L.; Zeng, Q.; Sethi, G.; Wang, L.; Lee, S. C.; Goh, B. C. Extracellular Vesicles, the Cornerstone of Next-Generation Cancer Diagnosis? *Semin. Cancer Biol.* **2021**, *74*, 105−120.

(11) Rehman, A.; Khan, M. A.; Saba, T.; Mehmood, Z.; Tariq, U.; Ayesha, N. Microscopic Brain Tumor Detection and Classification Using 3D CNN and Feature Selection Architecture. *Microsc. Res. Technol.* **2021**, *84*, 133−149.

(12) Zhou, S.; Yang, Y.; Wu, Y.; Liu, S. Review: Multiplexed Profiling of Biomarkers in Extracellular Vesicles for Cancer Diagnosis and Therapy Monitoring. *Anal. Chim. Acta* **2021**, *1175*, 338633.
(13) Moller, A.; Lobb, R. J. The Evolving Translational Potential of Small Extracellular Vesicles in Cancer. *Nat. Rev. Cancer* **2020**, *20*, 697−709.
(14) Su, C.; Zhang, J.; Yarden, Y.; Fu, L. The Key Roles of Cancer Stem Cell-Derived Extracellular Vesicles. *Signal Transduction Targeted Ther.* **2021**, *6*, 109.
(15) Yamazaki, S.; Ohka, F.; Hirano, M.; Shiraki, Y.; Motomura, K.; Tanahashi, K.; Tsujiuchi, T.; Motomura, A.; Aoki, K.; Shinjo, K.; Murofushi, Y.; Kitano, Y.; Maeda, S.; Kato, A.; Shimizu, H.; Yamaguchi, J.; Adilijiang, A.; Wakabayashi, T.; Saito, R.; Enomoto, A.; et al. Newly Established Patient-Derived Organoid Model of Intracranial Meningioma. *Neuro Oncol.* **2021**, *23*, 1936−1948.
(16) Zhao, Z.; Wijerathne, H.; Godwin, A. K.; Soper, S. A. Isolation and Analysis Methods of Extracellular Vesicles (EVs). *Extracell. Vesicles Circ. Nucl. Acids* **2021**, *2*, 80−103.
(17) Martins, A. M.; Ramos, C. C.; Freitas, D.; Reis, C. A. Glycosylation of Cancer Extracellular Vesicles: Capture Strategies, Functional Roles and Potential Clinical Applications. *Cells* **2021**, *10*, 109.
(18) Liangsupree, T.; Multia, E.; Riekkola, M. L. Modern Isolation and Separation Techniques for Extracellular Vesicles. *J. Chromatogr. A* **2021**, *1636*, 461773.
(19) Verweij, F. J.; Balaj, L.; Boulanger, C. M.; Carter, D. R. F.; Compeer, E. B.; D'Angelo, G.; El Andaloussi, S.; Goetz, J. G.; Gross, J. C.; Hyenne, V.; Kramer-Albers, E. M.; Lai, C. P.; Loyer, X.; Marki, A.; Momma, S.; Nolte-'t Hoen, E. N. M.; Pegtel, D. M.; Peinado, H.; Raposo, G.; Rilla, K.; et al. The Power of Imaging to Understand Extracellular Vesicle Biology *in vivo*. *Nat. Methods* **2021**, *18*, 1013−1026.
(20) LeClaire, M.; Gimzewski, J.; Sharma, S. A Review of the Biomechanical Properties of Single Extracellular Vesicles. *Nano Sel.* **2021**, *2*, 1−15.
(21) Russell, A. E.; Sneider, A.; Witwer, K. W.; Bergese, P.; Bhattacharyya, S. N.; Cocks, A.; Cocucci, E.; Erdbrugger, U.; Falcon-Perez, J. M.; Freeman, D. W.; Gallagher, T. M.; Hu, S.; Huang, Y.; Jay, S. M.; Kano, S. I.; Lavieu, G.; Leszczynska, A.; Llorente, A. M.; Lu, Q.; Mahairaki, V.; et al. Biological Membranes in EV Biogenesis, Stability, Uptake, and Cargo Transfer: an ISEV Position Paper Arising from the ISEV Membranes and EVs Workshop. *J. Extracell. Vesicles* **2019**, *8*, 1684862.
(22) Yanez-Mo, M.; Siljander, P. R.; Andreu, Z.; Zavec, A. B.; Borras, F. E.; Buzas, E. I.; Buzas, K.; Casal, E.; Cappello, F.; Carvalho, J.; Colas, E.; Cordeiro-da Silva, A.; Fais, S.; Falcon-Perez, J. M.; Ghobrial, I. M.; Giebel, B.; Gimona, M.; Graner, M.; Gursel, I.; Gursel, M.; et al. Biological Properties of Extracellular Vesicles and Their Physiological Functions. *J. Extracell. Vesicles* **2015**, *4*, 27066.
(23) Szatanek, R.; Baran, J.; Siedlar, M.; Baj-Krzyworzeka, M. Isolation of Extracellular Vesicles: Determining the Correct Approach (Review). *Int. J. Mol. Med.* **2015**, *36*, 11−17.
(24) Jeppesen, D. K.; Fenix, A. M.; Franklin, J. L.; Higginbotham, J. N.; Zhang, Q.; Zimmerman, L. J.; Liebler, D. C.; Ping, J.; Liu, Q.; Evans, R.; Fissell, W. H.; Patton, J. G.; Rome, L. H.; Burnette, D. T.; Coffey, R. J. Reassessment of Exosome Composition. *Cell* **2019**, *177*, 428−445.
(25) Contreras-Naranjo, J. C.; Wu, H. J.; Ugaz, V. M. Microfluidics for Exosome Isolation and Analysis: Enabling Liquid Biopsy for Personalized Medicine. *Lab Chip* **2017**, *17*, 3558−3577.
(26) Peterson, M. F.; Otoc, N.; Sethi, J. K.; Gupta, A.; Antes, T. J. Integrated Systems for Exosome Investigation. *Methods* **2015**, *87*, 31−45.
(27) Liu, C.; Zhao, J.; Tian, F.; Chang, J.; Zhang, W.; Sun, J. Lambda-DNA- and Aptamer-Mediated Sorting and Analysis of Extracellular Vesicles. *J. Am. Chem. Soc.* **2019**, *141*, 3817−3821.
(28) Liu, C.; Guo, J.; Tian, F.; Yang, N.; Yan, F.; Ding, Y.; Wei, J.; Hu, G.; Nie, G.; Sun, J. Field-Free Isolation of Exosomes from Extracellular Vesicles by Microfluidic Viscoelastic Flows. *ACS Nano* **2017**, *11*, 6968−6976.
(29) Yasui, T.; Paisrisarn, P.; Yanagida, T.; Konakade, Y.; Nakamura, Y.; Nagashima, K.; Musa, M.; Thiodorus, I. A.; Takahashi, H.; Naganawa, T.; Shimada, T.; Kaji, N.; Ochiya, T.; Kawai, T.; Baba, Y. Molecular Profiling of Extracellular Vesicles *via* Charge-Based Capture Using Oxide Nanowire Microfluidics. *Biosens. Bioelectron.* **2021**, *194*, 113589.
(30) Yasui, T.; Yanagida, T.; Ito, S.; Konakade, Y.; Takeshita, D.; Naganawa, T.; Nagashima, K.; Shimada, T.; Kaji, N.; Nakamura, Y.; Thiodorus, I. A.; He, Y.; Rahong, S.; Kanai, M.; Yukawa, H.; Ochiya, T.; Kawai, T.; Baba, Y. Unveiling Massive Numbers of Cancer-Related Urinary-MicroRNA Candidates *via* Nanowires. *Sci. Adv.* **2017**, *3*, No. e1701133.
(31) Kitano, Y.; Aoki, K.; Ohka, F.; Yamazaki, S.; Motomura, K.; Tanahashi, K.; Hirano, M.; Naganawa, T.; Iida, M.; Shiraki, Y.; Nishikawa, T.; Shimizu, H.; Yamaguchi, J.; Maeda, S.; Suzuki, H.; Wakabayashi, T.; Baba, Y.; Yasui, T.; Natsume, A. Urinary MicroRNA-Based Diagnostic Model for Central Nervous System Tumors Using Nanowire Scaffolds. *ACS Appl. Mater. Interfaces* **2021**, *13*, 17316−17329.
(32) Paisrisarn, P.; Yasui, T.; Zhu, Z.; Klamchuen, A.; Kasamechonchung, P.; Wutikhun, T.; Yordsri, V.; Baba, Y. Tailoring ZnO Nanowire Crystallinity and Morphology for Label-Free Capturing of Extracellular Vesicles. *Nanoscale* **2022**, *14*, 4484−4494.
(33) Bordanaba-Florit, G.; Royo, F.; Kruglik, S. G.; Falcon-Perez, J. M. Using Single-Vesicle Technologies to Unravel the Heterogeneity of Extracellular Vesicles. *Nat. Protoc.* **2021**, *16*, 3163−3185.
(34) Hilton, S. H.; White, I. M. Advances in the Analysis of Single Extracellular Vesicles: a Critical Review. *Sens. Actuators Rep.* **2021**, *3*, 100052.
(35) Shao, H.; Im, H.; Castro, C. M.; Breakefield, X.; Weissleder, R.; Lee, H. New Technologies for Analysis of Extracellular Vesicles. *Chem. Rev.* **2018**, *118*, 1917−1950.
(36) Banaei, N.; Moshfegh, J.; Kim, B. Surface Enhanced Raman Spectroscopy-Based Immunoassay Detection of Tumor-Derived Extracellular Vesicles to Differentiate Pancreatic Cancers from Chronic Pancreatitis. *J. Raman Spectrosc.* **2021**, *52*, 1810−1819.
(37) Tan, K. L.; Chia, W. C.; How, C. W.; Tor, Y. S.; Show, P. L.; Looi, Q. H. D.; Foo, J. B. Benchtop Isolation and Characterisation of Small Extracellular Vesicles from Human Mesenchymal Stem Cells. *Mol. Biotechnol.* **2021**, *63*, 780−791.
(38) Liang, K.; Liu, F.; Fan, J.; Sun, D.; Liu, C.; Lyon, C. J.; Bernard, D. W.; Li, Y.; Yokoi, K.; Katz, M. H.; Koay, E. J.; Zhao, Z.; Hu, Y. Nanoplasmonic Quantification of Tumour-Derived Extracellular Vesicles in Plasma Microsamples for Diagnosis and Treatment Monitoring. *Nat. Biomed. Eng.* **2017**, *1*, 21.
(39) Bandu, R.; Oh, J. W.; Kim, K. P. Mass Spectrometry-Based Proteome Profiling of Extracellular Vesicles and Their Roles in Cancer Biology. *Exp. Mol. Med.* **2019**, *51*, 1−10.
(40) Dragovic, R. A.; Gardiner, C.; Brooks, A. S.; Tannetta, D. S.; Ferguson, D. J.; Hole, P.; Carr, B.; Redman, C. W.; Harris, A. L.; Dobson, P. J.; Harrison, P.; Sargent, I. L. Sizing and Phenotyping of Cellular Vesicles Using Nanoparticle Tracking Analysis. *Nanomedicine* **2011**, *7*, 780−788.
(41) Eitan, E.; Green, J.; Bodogai, M.; Mode, N. A.; Baek, R.; Jorgensen, M. M.; Freeman, D. W.; Witwer, K. W.; Zonderman, A. B.; Biragyn, A.; Mattson, M. P.; Noren Hooten, N.; Evans, M. K. Age-Related Changes in Plasma Extracellular Vesicle Characteristics and Internalization by Leukocytes. *Sci. Rep.* **2017**, *7*, 1342.
(42) Takai, H.; Kato, A.; Nakamura, T.; Tachibana, T.; Sakurai, T.; Nanami, M.; Suzuki, M. The Importance of Characterization of FITC-Labeled Antibodies Used in Tissue Cross-Reactivity Studies. *Acta Histochem.* **2011**, *113*, 472−476.
(43) Colombo, M.; Raposo, G.; Thery, C. Biogenesis, Secretion, and Intercellular Interactions of Exosomes and Other Extracellular Vesicles. *Annu. Rev. Cell Dev. Biol.* **2014**, *30*, 255−289.


https://doi.org/10.1021/acsnano.2c08526
*ACS Nano* 2023, 17, 2235−2244

(44) Bobrie, A.; Colombo, M.; Raposo, G.; Thery, C. Exosome Secretion: Molecular Mechanisms and Roles in Immune Responses. *Traffic* **2011**, *12*, 1659−1668.
(45) Im, H.; Shao, H.; Park, Y. I.; Peterson, V. M.; Castro, C. M.; Weissleder, R.; Lee, H. Label-Free Detection and Molecular Profiling of Exosomes with a Nano-Plasmonic Sensor. *Nat. Biotechnol.* **2014**, *32*, 490−495.
(46) Zhang, P.; Zhou, X.; He, M.; Shang, Y.; Tetlow, A. L.; Godwin, A. K.; Zeng, Y. Ultrasensitive Detection of Circulating Exosomes with a 3D-Nanopatterned Microfluidic Chip. *Nat. Biomed. Eng.* **2019**, *3*, 438−451.
(47) Lo, T. W.; Zhu, Z.; Purcell, E.; Watza, D.; Wang, J.; Kang, Y. T.; Jolly, S.; Nagrath, D.; Nagrath, S. Microfluidic Device for High-Throughput Affinity-Based Isolation of Extracellular Vesicles. *Lab Chip* **2020**, *20*, 1762−1770.
(48) Zhang, P.; Wu, X.; Gardashova, G.; Yang, Y.; Zhang, Y.; Xu, L.; Zeng, Y. Molecular and Functional Extracellular Vesicle Analysis Using Nanopatterned Microchips Monitors Tumor Progression and Metastasis. *Sci. Transl. Med.* **2020**, *12*, No. eaaz2878.
(49) Takeuchi, T.; Mori, K.; Sunayama, H.; Takano, E.; Kitayama, Y.; Shimizu, T.; Hirose, Y.; Inubushi, S.; Sasaki, R.; Tanino, H. Antibody-Conjugated Signaling Nanocavities Fabricated by Dynamic Molding for Detecting Cancers Using Small Extracellular Vesicle Markers from Tears. *J. Am. Chem. Soc.* **2020**, *142*, 6617−6624.
(50) Mateescu, B.; Kowal, E. J.; van Balkom, B. W.; Bartel, S.; Bhattacharyya, S. N.; Buzas, E. I.; Buck, A. H.; de Candia, P.; Chow, F. W.; Das, S.; Driedonks, T. A.; Fernandez-Messina, L.; Haderk, F.; Hill, A. F.; Jones, J. C.; Van Keuren-Jensen, K. R.; Lai, C. P.; Lasser, C.; Liegro, I. D.; Lunavat, T. R.; et al. Obstacles and Opportunities in the Functional Analysis of Extracellular Vesicle RNA - an ISEV Position Paper. *J. Extracell. Vesicles* **2017**, *6*, 1286095.
(51) An, Z.; Aksoy, O.; Zheng, T.; Fan, Q. W.; Weiss, W. A. Epidermal Growth Factor Receptor and EGFRvIII in Glioblastoma: Signaling Pathways and Targeted Therapies. *Oncogene* **2018**, *37*, 1561−1575.
(52) Kim, K.; Brush, J. M.; Watson, P. A.; Cacalano, N. A.; Iwamoto, K. S.; McBride, W. H. Epidermal Growth Factor Receptor vIII Expression in U87 Glioblastoma Cells Alters Their Proteasome Composition, Function, and Response to Irradiation. *Mol. Cancer Res.* **2008**, *6*, 426−434.
(53) Ohno, M.; Natsume, A.; Ichiro Iwami, K.; Iwamizu, H.; Noritake, K.; Ito, D.; Toi, Y.; Ito, M.; Motomura, K.; Yoshida, J.; Yoshikawa, K.; Wakabayashi, T. Retrovirally Engineered T-Cell-Based Immunotherapy Targeting Type III Variant Epidermal Growth Factor Receptor, a Glioma-Associated Antigen. *Cancer Sci.* **2010**, *101*, 2518−2524.
(54) Jensen, C.; Teng, Y. Is It Time to Start Transitioning from 2D to 3D Cell Culture? *Front. Mol. Biosci.* **2020**, *7*, 33.
(55) Klein, E.; Hau, A. C.; Oudin, A.; Golebiewska, A.; Niclou, S. P. Glioblastoma Organoids: Pre-Clinical Applications and Challenges in the Context of Immunotherapy. *Front. Oncol.* **2020**, *10*, 604121.
(56) Diao, W.; Tong, X.; Yang, C.; Zhang, F.; Bao, C.; Chen, H.; Liu, L.; Li, M.; Ye, F.; Fan, Q.; Wang, J.; Ou-Yang, Z. C. Behaviors of Glioblastoma Cells in *in vitro* Microenvironments. *Sci. Rep.* **2019**, *9*, 85.
(57) Kahlert, U. D.; Joseph, J. V.; Kruyt, F. A. E. Emt- and Met-Related Processes in Nonepithelial Tumors: Importance for Disease Progression, Prognosis, and Therapeutic Opportunities. *Mol. Oncol.* **2017**, *11*, 860−877.
(58) Khattab, A. Z.; Ahmed, M. I.; Fouad, M. A.; Essa, W. A. Significance of P53 and CD31 in Astrogliomas. *Med. Oncol.* **2009**, *26*, 86−92.
(59) Singh, A.; Settleman, J. Emt, Cancer Stem Cells and Drug Resistance: an Emerging Axis of Evil in the War on Cancer. *Oncogene* **2010**, *29*, 4741−4751.
(60) Jeppesen, D. K.; Hvam, M. L.; Primdahl-Bengtson, B.; Boysen, A. T.; Whitehead, B.; Dyrskjot, L.; Orntoft, T. F.; Howard, K. A.; Ostenfeld, M. S. Comparative Analysis of Discrete Exosome Fractions Obtained by Differential Centrifugation. *J. Extracell. Vesicles* **2014**, *3*, 25011.
(61) Ishihara, R.; Katagiri, A.; Nakajima, T.; Matsui, R.; Hosokawa, K.; Maeda, M.; Tomooka, Y.; Kikuchi, A. Design of a Sensitive Extracellular Vesicle Detection Method Utilizing a Surface-Functionalized Power-Free Microchip. *Membranes* **2022**, *12*, 679.
(62) Momenbeitollahi, N.; Aggarwal, R.; Strohle, G.; Bouriayee, A.; Li, H. Extracellular Vesicle (EV) Dot Blotting for Multiplexed EV Protein Detection in Complex Biofluids. *Anal. Chem.* **2022**, *94*, 7368−7374.
(63) Jiang, Q.; Liu, Y.; Wang, L.; Adkins, G. B.; Zhong, W. Rapid Enrichment and Detection of Extracellular Vesicles Enabled by CuS-Enclosed Microgels. *Anal. Chem.* **2019**, *91*, 15951−15958.
(64) Daaboul, G. G.; Gagni, P.; Benussi, L.; Bettotti, P.; Ciani, M.; Cretich, M.; Freedman, D. S.; Ghidoni, R.; Ozkumur, A. Y.; Piotto, C.; Prosperi, D.; Santini, B.; Unlu, M. S.; Chiari, M. Digital Detection of Exosomes by Interferometric Imaging. *Sci. Rep.* **2016**, *6*, 37246.
(65) Xia, Y.; Liu, M.; Wang, L.; Yan, A.; He, W.; Chen, M.; Lan, J.; Xu, J.; Guan, L.; Chen, J. A Visible and Colorimetric Aptasensor Based on DNA-Capped Single-Walled Carbon Nanotubes for Detection of Exosomes. *Biosens. Bioelectron.* **2017**, *92*, 8−15.

## Recommended by ACS

**Integrated SERS-Vertical Flow Biosensor Enabling Multiplexed Quantitative Profiling of Serological Exosomal Proteins in Patients for Accurate Breast Cancer Subtyping**
Xiaoming Su, Ming Li, *et al.*
FEBRUARY 09, 2023
ACS NANO
READ

**Robust Acute Pancreatitis Identification and Diagnosis: RAPIDx**
Qingfu Zhu, Fei Liu, *et al.*
MARCH 29, 2023
ACS NANO
READ

**Nanopore-Based Fingerprint Immunoassay Based on Rolling Circle Amplification and DNA Fragmentation**
Xinqi Kang, Meni Wanunu, *et al.*
MARCH 06, 2023
ACS NANO
READ

**Purification Analysis, Intracellular Tracking, and Colocalization of Extracellular Vesicles Using Atomic Force and 3D Single-Molecule Localization Microscopy**
Sujitha Puthukodan, Jaroslaw Jacak, *et al.*
MARCH 31, 2023
ANALYTICAL CHEMISTRY
READ

Get More Suggestions >


https://doi.org/10.1021/acsnano.2c08526
*ACS Nano* 2023, 17, 2235−2244